https://ntrs.nasa.gov/search.jsp?R=19940025271 2018-04-20T14:35:01+00:00Z

N94-29775

A Sub-cm Micromachined Electron Microscope

A.D. Feinerman, D.A. Crewe, D.C. Perng, and S.E. Shoaf

Microfabrication Applications Laboratory, Electrical Engineering and Computer Science Department (M/C 154), University of Illinois at Chicago, Box 4348, Chicago, IL 60607

A.V. Crewe

Enrico Fermi Institute and the Department of Physics, University of Chicago, 5640 S. Ellis Ave., Chicago, IL 60637

A new approach for fabricating macroscopic (~10x10x10mm^3) structures with micron accuracy has been developed. This approach combines the precision of semiconductor processing and fiber optic technologies. A (100) silicon wafer is anisotropically etched to create four orthogonal v-grooves and an aperture on each 10x12mm die. Precision 308μm optical fibers are sandwiched between the die to align the v-grooves. The fiber is then anodically bonded to the die above and below it. This procedure is repeated to create thick structures and a stack of 5 or 6 die will be used to create a miniature scanning electron microscope (MSEM). See Figure 1. Two die in the structure will have a segmented electrode to deflect the beam and correct for astigmatism. The entire structure is UHV compatible.

The performance of an SEM improves as its length is reduced[1] and a sub-cm 2keV MSEM with a field emission source should have approximately 1nm resolution[2]. A low voltage high resolution MSEM would be useful for the examination of biological specimens and semiconductors with a minimum of damage. The first MSEM will be tested with existing 6μm thermionic sources.[3]

Reprinted with permission from the *Journal of Vacuum Science Technology A*, vol. 10, no. 4, part 1, July-August 1992, pp. 611-616.

PRECEDING PAGE BLANK NOT FILMED

In the future a micromachined field emission source will be used. The stacking technology presented in this paper can produce an array of MSEMs 1 to 30mm in length with a 1mm or larger period. A key question being addressed by this research is the optimum size for a low voltage MSEM which will be determined by the required spatial resolution, field of view, and working distance.

I. INTRODUCTION

An MSEM can operate in previously inaccessible locations. For example, an MSEM on a portable boom could inspect the deterioration of a fusion reactor's walls from plasma and radiation damage without disassembling the reactor to bring its sections to the microscopy laboratory. As a second example the scanning tunneling microscope (STM) has atomic resolution but the operator has difficulty locating interesting features on the specimen with a single choice of magnification. An MSEM with only 1000X magnification and a 100μm field of view observing the STM tip would alleviate this problem.

The technology used to make a single MSEM will also make an array of MSEMs for direct write lithography. Matching the MSEM array period with that of the substrate would simplify the drive electronics. This MSEM array would also be useful for a rapid inspection of specimens. Once a defect had been located similar spots on adjacent sections of the specimen could be quickly examined without a mechanical translation.

II. MICROSCOPE STRUCTURE

The silicon die used in this research are from 3-in. 3-5 ohm-cm (100) n-type silicon wafers 381μm thick (Figure 2). The structure is designed to have the fibers rest on the etched v-groove surface as opposed to resting on the

groove's edges (Figure 3). The relationship between groove width (W), fiber diameter (D), and gap between silicon die is given by the following equations[4] where $\theta = \cos^{-1}(\sqrt{2/3}) = 35.26°$.

$$\text{if } D \leq \frac{W}{\cos(\theta)} \qquad \text{Gap} = \frac{D}{\sin(\theta)} - \frac{W}{\tan(\theta)} \qquad (1)$$

$$\text{if } D \geq \frac{W}{\cos(\theta)} \qquad \text{Gap} = \sqrt{D^2 - W^2} \qquad (2)$$

The glass deforms up to 1.6μm during anodic bonding to silicon[5,6]. This deformation will increase the fiber/silicon contact area and the increase will be larger if the contact point is below the silicon wafer surface[7] (Figure 3a). The bond strength between the fiber and the silicon will increase as the contact area increases. Die have been stacked with 308 and 450μm diameter fibers in 270μm wide grooves yielding 152 and 360μm gaps between the silicon die respectively. Attempts to bond 510μm fibers into the 270μm grooves have not been successful, possibly due to the small fiber/silicon contact area.

The wafers were cleaned and then oxidized in steam at 900°C to grow 40nm of SiO_2. A 200nm Si_3N_4 layer was then deposited over the SiO_2 in an LPCVD reactor. The top of the wafers were coated with HMDS primer and Shipley 813 photoresist. Rectangular 270x7000μm^2 and square 740μm windows were opened in the photoresist after aligning the pattern to the wafer flat. The Si_3N_4 was etched for 50 seconds in a Tegal 803 plasma etcher; then the photoresist was removed. The bottom surface of the wafer was aligned to the etched features on top of the wafer with an infrared aligner, then plasma etched. The exposed oxide was removed with a 2 minute immersion in buffered HF acid, the wafers were then immersed in a quartz reflux system containing an anisotropic etching solution (44% by weight KOH in H_2O at 82°C). This solution etches the

silicon (100) direction 400 times faster than the (111) direction[8] and has a negligible etch rate for Si_3N_4.[9] The wafers were kept in this solution for 5.5 hours until the KOH solution etched through the wafer and a 740μm square opening formed a 200μm square aperture on the opposite side of the wafer. The 270x7000μm^2 openings formed v-grooves 191μm deep to hold 6mm long fibers. The Si_3N_4 etch mask was then removed with a 10 minute immersion in 50% HF acid followed by a 5 minute deionized H_2O rinse. In the future a boron etch stop will be used to create circular apertures using a process similar to that which creates micromachined ink jet nozzles.[10] The wafers were then cut into 10x12mm die using a MicroAutomation 1006A dicing saw and cleaned. The die were aligned and anodically bonded[7] together with 308μm duran fibers as shown in (Figures 4 and 5). Duran or pyrex is chosen because their thermal expansion coefficients of 3.2×10^{-6}/°C closely match that of silicon at 2.6×10^{-6}/°C Both glasses have nearly identical chemical composition and are trademarks of Schott and Corning respectively. A second advantage is that the glasses can be attached to silicon at 250°C with a bond strength of 350psi[11]. The bond is strong enough (1.0±0.5 pounds) to allow the die to be wire bonded. A stack of six die with 152μm gaps forms an electron optical column 3mm long. The column is mounted on an Airpax 1.1"x1.1" glass sealed 18 pin header which is attached to a standard vacuum flange (Figure 6).

The accuracy of the stacking technique is limited by the precision of the glass fibers, silicon die, and v-groove etching. Optical fibers drawn with laser micrometer control have a diameter tolerance of ±0.1%/km of fiber[12] or ±0.3μm/km for a 308μm fiber. A kilometer of fiber would provide enough material for several thousand microscopes. The total indicated runout (TIR), which is defined as the maximum surface deviation, on a 10x12mm^2 double polished silicon die is much less than 1μm. The etched v-groove (111)

ORIGINAL PAGE IS
OF POOR QUALITY

surfaces also have less than 1μm of TIR. At present the overall accuracy of the column is limited by the ±5μm infrared alignment of etched features in the top and bottom surfaces of the silicon die. This accuracy will be improved by initially etching a feature through the silicon wafer and aligning each surface to this feature. The stacking technique should achieve submicron accuracy.

The relationship between operating voltage and minimum column length is being explored assuming a maximum electric field of 10kV/mm[1]. Stacking with fibers D μm in diameter, the maximum gap between the silicon die is 0.577xD if the fiber rests inside the v-groove and has a contact point at the silicon wafer surface. The silicon is etched at least 0.211xD to seat the fiber and 0.577xD if the v-groove completes. The die must be thicker than the etch depth for structural integrity and the minimum die thickness is assumed to be the fiber diameter. The length of a six layer column with the maximum gap between thin layers is 6xD + 5x0.577xD. A 1mm column with 640 volts between layers (64μm gaps) can be fabricated from 110μm fibers and wafers.

III. ELECTRON SOURCE

The resolution of an electron microscope improves as the source brightness is increased. It has been predicted[1] that a micromachined field emission source can be 2 to 3 orders of magnitude brighter than a conventional field emission source. Micromachined and conventional field emission sources will be integrated into a stacked structure to verify their performance. Initial testing of the column will be carried out with a low brightness micromachined thermionic emitter. This will give a rough test of the column performance and measure the maximum electric field that can be sustained between silicon layers separated by 30 to 300μm gaps.

The micromachined thermionic emitters[3] are fabricated on a silicon wafer (Figure 7). The wafers are oxidized in steam at 1100°C to grow 1μm of SiO_2. The SiO_2 layer electrically isolates the filament from the substrate. A 1μm tungsten layer is then sputtered on top of the SiO_2 and patterned with a wet etchant. The SiO_2 below the tungsten film is removed in buffered HF for 20 to 50 minutes depending on the filament width. The wafer is then immersed in KOH to etch 10μm of silicon to avoid any possible contact between the substrate and the heated filament. A filament that emitted 10namps for 60 minutes is shown in (Figure 8).

IV. ELECTRON OPTICAL CALCULATIONS OF EINZEL LENS AND DEFLECTOR

Preliminary electron optical calculations of the Einzel lenses in (Figure 9) were performed as follows. Previous experience indicated that the number of mesh points in the axial direction is more critical than in the radial direction and a grid (or mesh) was chosen with 701 lines along the optical axis and 50 lines in the radial direction. The electrodes themselves are defined in the grid as equipotential surfaces that will have fixed values during the calculation. The potential far from the optical axis is assumed to vary linearly between the electrodes. The calculation assumes cylindrical symmetry which will be justified if the circular apertures in the die are 10 times smaller than the square openings (Figure 2). The computational mesh is finer near the apertures where the potential is expected to vary faster. The next step is to solve Laplace's equation for the defined mesh using the finite difference method to obtain the potential on the axis. The rectangular grid is transformed to a triangular mesh by connecting the corners of the rectangles. The vertices of the triangles are the points that are assigned a potential each time through an iteration, with the final convergence solution

ORIGINAL PAGE IS
OF POOR QUALITY

varying by no more than one part in 10^{-8} from the previous solution. Paraxial rays are traced with a fourth order Runga-Kutta routine after the axial potential is calculated. The input to the routine is simply the initial position and slope of the electron, so the position and size of the source and a beam defining aperture can be included in the calculation.

The following parameters can be changed in the design of our three element micromachined Einzel lens: thermionic electron source size, thickness and spacing of the electrodes, aperture size and thickness, and position of the aperture on the electrode (leading or trailing edge). See Figure 9. The first aperture size defines the maximum angle of accepted emission. The second aperture diameter defines the potential necessary to focus over a desired range. The third aperture has little effect as long as it is on the order of the first aperture size. The electrode spacing is given by equation (1).

The optical properties (aberration coefficients, potential range for desired focal points, etc.) of two lenses can be meaningfully compared only if their first order focal positions are identical. Two implementations of an electrode structure designed to give a good range of focal positions (from the exit of the gun out to infinity, for instance) were investigated as shown in Figure 9. The individual electrode contributions to the axial potential and a ray trace comparison between the two lenses are shown in (Figures 10 and 11). It appears that the more gradual focusing effect of the second electrode with the aperture on a trailing instead of a leading edge is the more desirable design.

The final two electrodes in Figure 9 are segmented to correct for astigmatism and to simulate a parallel plate deflector (Figure 12). The beam deflection angle is given by $\tan(\alpha) = (LE_{tr})/(2V)$, where L is the axial

ORIGINAL PAGE IS
OF POOR QUALITY

length of the deflector (gap between silicon die), V is the beam energy as it enters the deflector and E_{tr} is the uniform transverse electric field created between the deflector plates. A field of view of 100μm requires a 0.57° deflection with a 5mm working distance. A 1kV beam is deflected 0.57° with a transverse field of 130V/mm and an L of 0.152mm.

V. CONCLUSIONS

A new technique has been developed for creating thick three dimensional structures with an accuracy approaching 1μm in three directions. The technique combines semiconductor processing and fiber optic technology. The method is being used to fabricate several versions of a miniature SEM (MSEM) 2.5 to 3mm thick from five or six silicon die. The entire structure is assembled by hand and is very rugged. The fabrication method presented in this paper can produce a six layer structure 1mm long using 110μm silicon wafers and glass fibers with 640 volts between layers (Figure 1b). The method could also fabricate arrays of MSEMs for direct write lithography and wafer inspection. Three advantages of an MSEM would be: reduction in column and vacuum hardware cost, ease of operation as all the critical components are permanently aligned to the electron optical axis, and, due to its small size, the ability to observe specimens in previously inaccessible locations.

ACKNOWLEDGMENTS

This research was supported by an NSF RIA 9009842 "Microfabrication of Electron Optical Components," a State of Illinois Technology Challenge Grant "Microfabrication Applications Laboratory," and Monolithic Sensors Inc. "Stacking of Pressure Transducers." The authors are indebted to Professor Max Epstein and Casey Cott of Northwestern University Electrical Engineering

ORIGINAL PAGE IS
OF POOR QUALITY

Department for supplying the pyrex fiber and to Dr. Walter Siegmund of Schott Fiber Optic for supplying the duran fiber. Special thanks to Dr. Peter Loeppert and James Branthaver of Monolithic Sensors for guiding and assisting with the silicon processing, Mr. Wayne Ahlstrom of Mallincrodt for chemical etching assistance, Mr. Bryan Maurantonio of MEMC for insights on silicon wafer technology, Mr. John Schnecker of Buehler for polishing assistance, and to Anthony Cocco for several helpful suggestions.

References

1 T.H.P.Chang, D.P. Kern, and D.P. Muray, J. Vac. Sci. Technol. B **8**, 1698 (1990).

2 A.V. Crewe, University of Chicago, "A Sub-Miniature Integrated Electron Microscope," private communication (1990).

3 D.C. Perng, D.A. Crewe, and A.D. Feinerman, J. Micromech. Microeng. 2 no. 1, in press (1992).

4 M.A. Mentzer, in "Principles of Optical Circuit Engineering", Appendix IV, p301-307, M. Dekker, New York (1990).

5 D.E. Carlson, J. Amer. Ceram. Soc. **57**, 291 (1974).

6 D.E. Carlson, K.W. Hang, and G.F. Stockdale, J. Amer. Ceram. Soc. **57**, 295 (1974).

7 A.D. Feinerman, S.E. Shoaf, and D.A. Crewe, "Precision Aligning and Bonding of Silicon Die," Proceedings of the 180th ECS Conference, Phoenix, AZ, October, 1991.

8 K.E. Petersen, Proceedings of the IEEE **70**, 422 (1982).

9 K.E. Bean, IEEE Trans. on Electron Devices **ED-25**, 1185 (1978).

10 E. Bassous, IEEE Trans. on Electron Devices **ED-25**, 1178 (1978).

11 G. Wallis, and D.I. Pomerantz, J. Appl. Phys. **40**, 3946 (1969).

12 J. Gowar, in "Optical Communication systems," p99, Prentice Hall International, London (1984).

ORIGINAL PAGE IS
OF POOR QUALITY

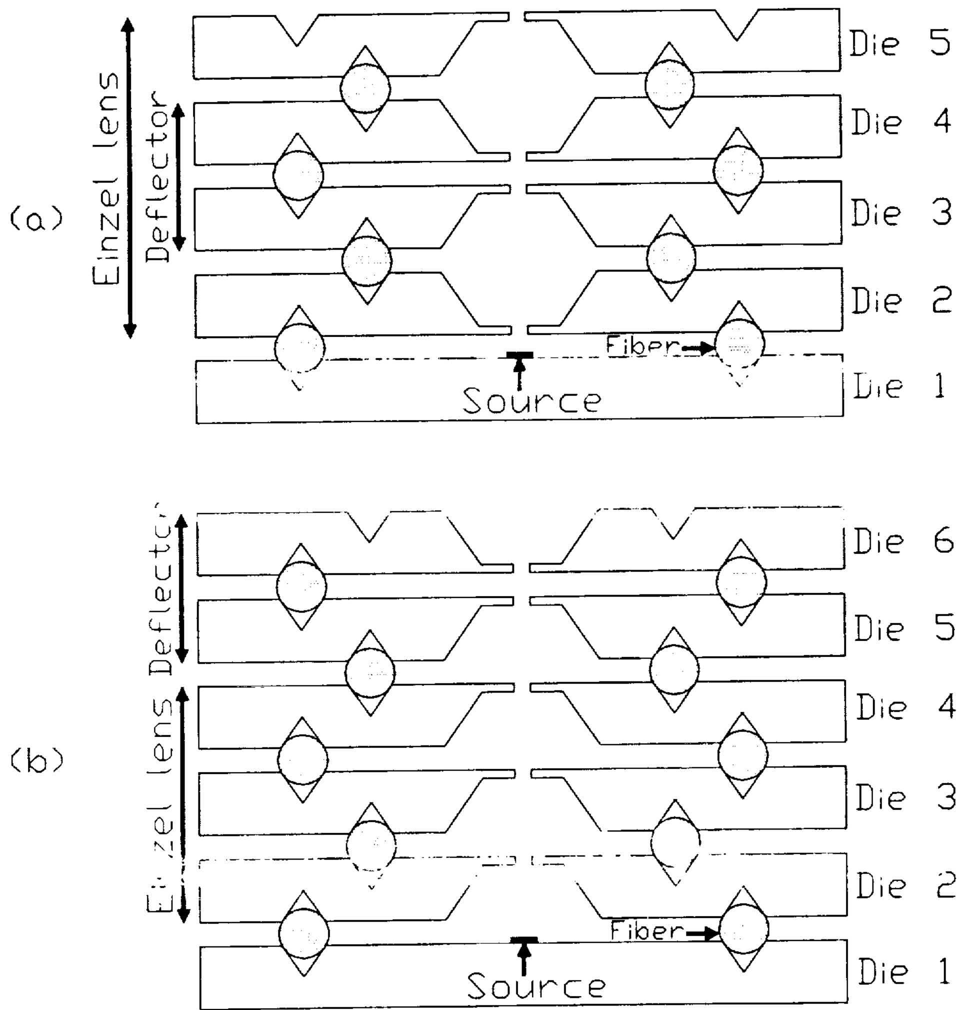

Figure 1

Silicon die are stacked with glass fibers that align and bond to the dies' v-grooves. The v-grooves are staggered to increase the die strength. The top and bottom surfaces of each die are optically aligned during fabrication. The stacking method is versatile and several electron optical columns will be fabricated and studied. Each column consists of a micromachined thermionic or field emission electron source, an Einzel lens that accelerates and focuses the emitted electrons, and two die with segmented electrodes to deflect the beam.

a) Deflecting the electron beam inside a decelerating Einzel lens increases the field of view and working distance at the expense of circuit complexity.
b) The beam is focused by a three electrode Einzel lens and then deflected.

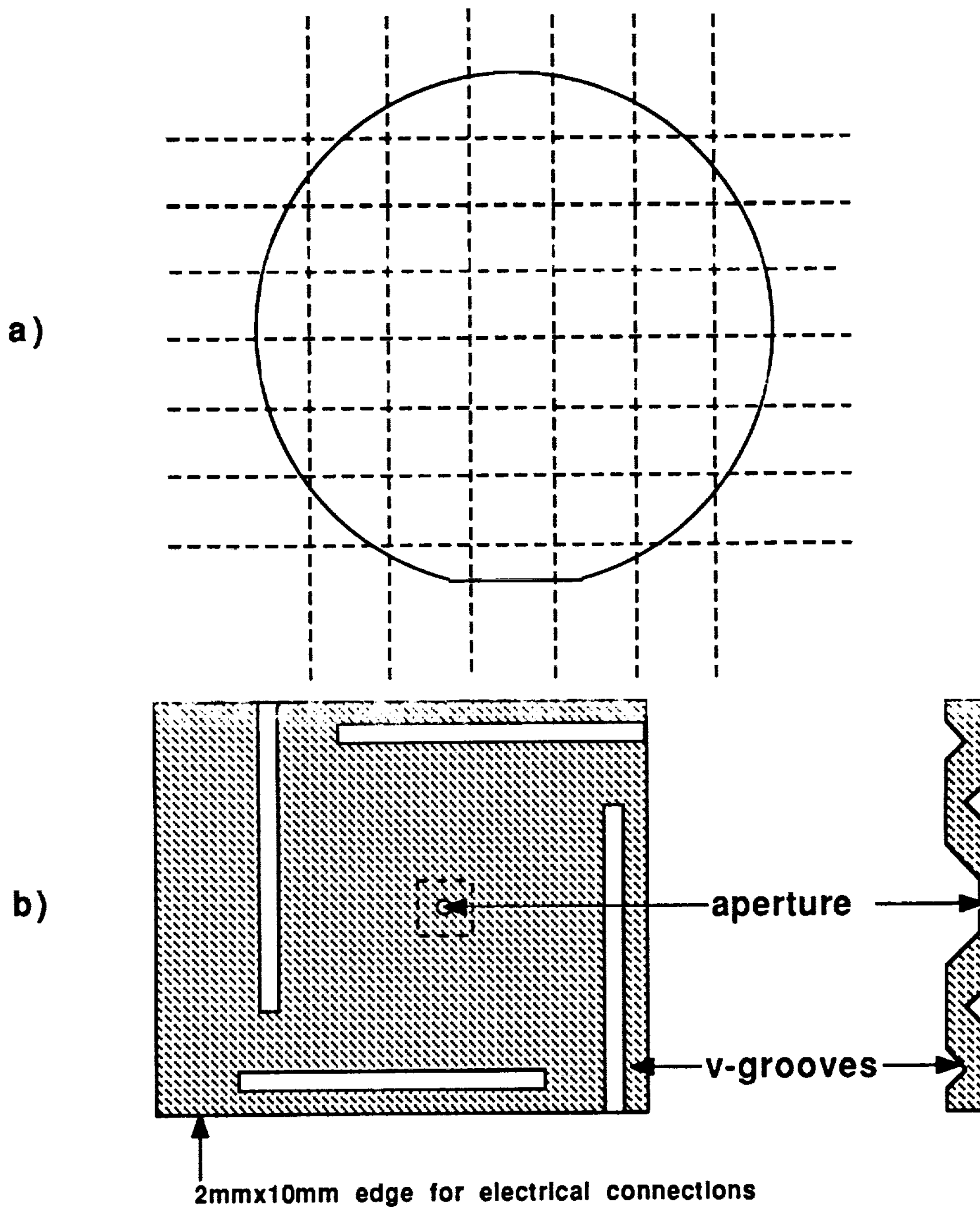

Figure 2

a) A silicon wafer is processed to produce 26 10x12mm die.
b) Each die contains 4 v-grooves and a membrane with a circular aperture. Entire wafers could be stacked with this technique by etching four v-grooves around the perimeter of the wafer. In this manner an array of MSEMs will be fabricated with a period of 1mm or larger.

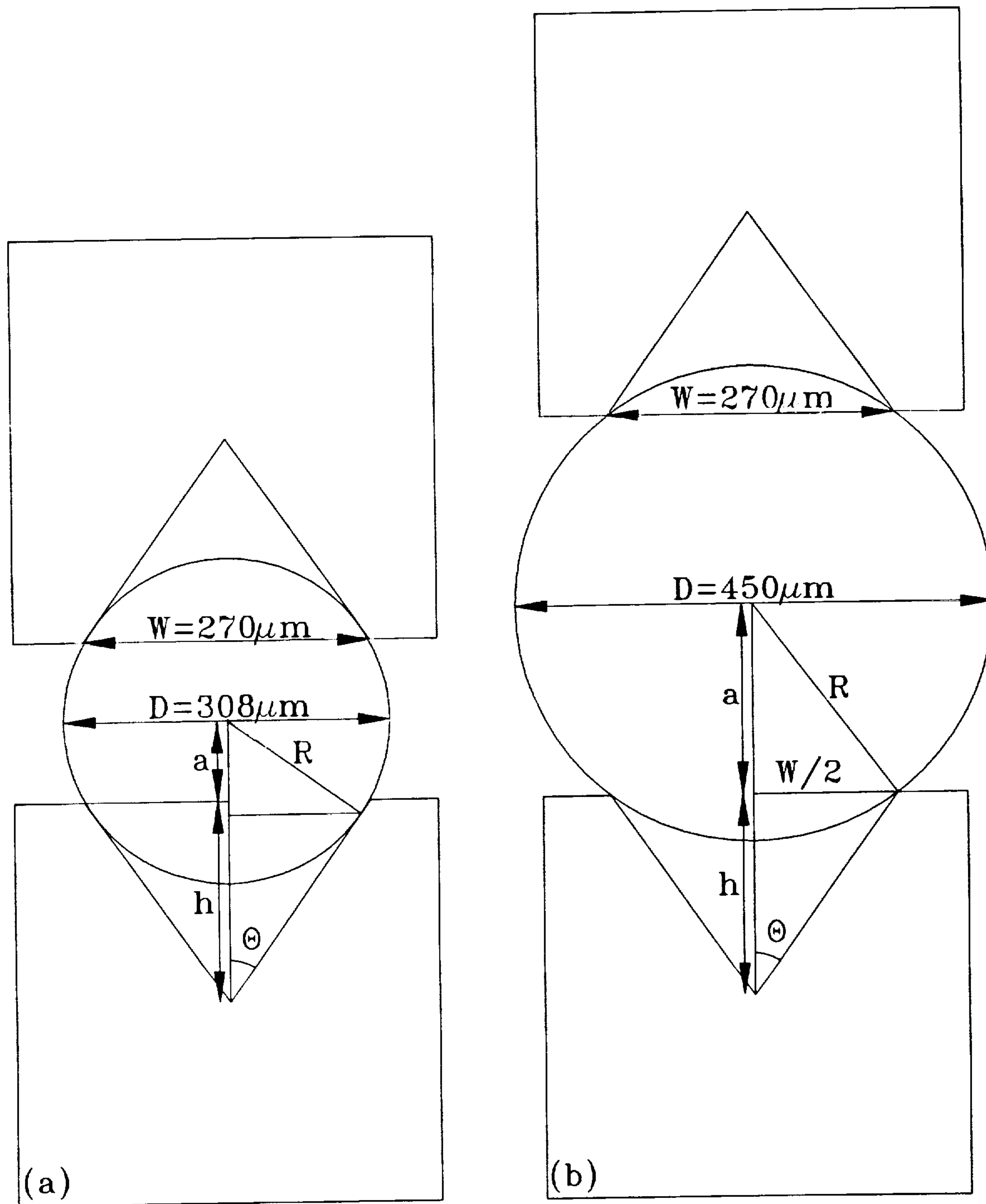

Figure 3

The gap between silicon die (2a) is determined by the v-groove width (W), and the fiber diameter (D=2R). The half angle of the v-groove is $\theta=35.26°$, and the depth is $h=W/\sqrt{2}$.

a) The center of a 308μm fiber is positioned 76μm above a 270μm v-groove. The fiber contacts the silicon 13μm below the silicon wafer surface.

b) The center of a 450μm fiber is positioned 180μm above a 270μm v-groove. The fiber contacts the silicon at the silicon wafer surface and rests on the groove's edges.

Figure 4

Two silicon die are aligned and anodically bonded to a 308μm diameter duran fiber. The die are aligned to within the accuracy of the optical micrograph ~±2μm. The separation between the die is 152μm.

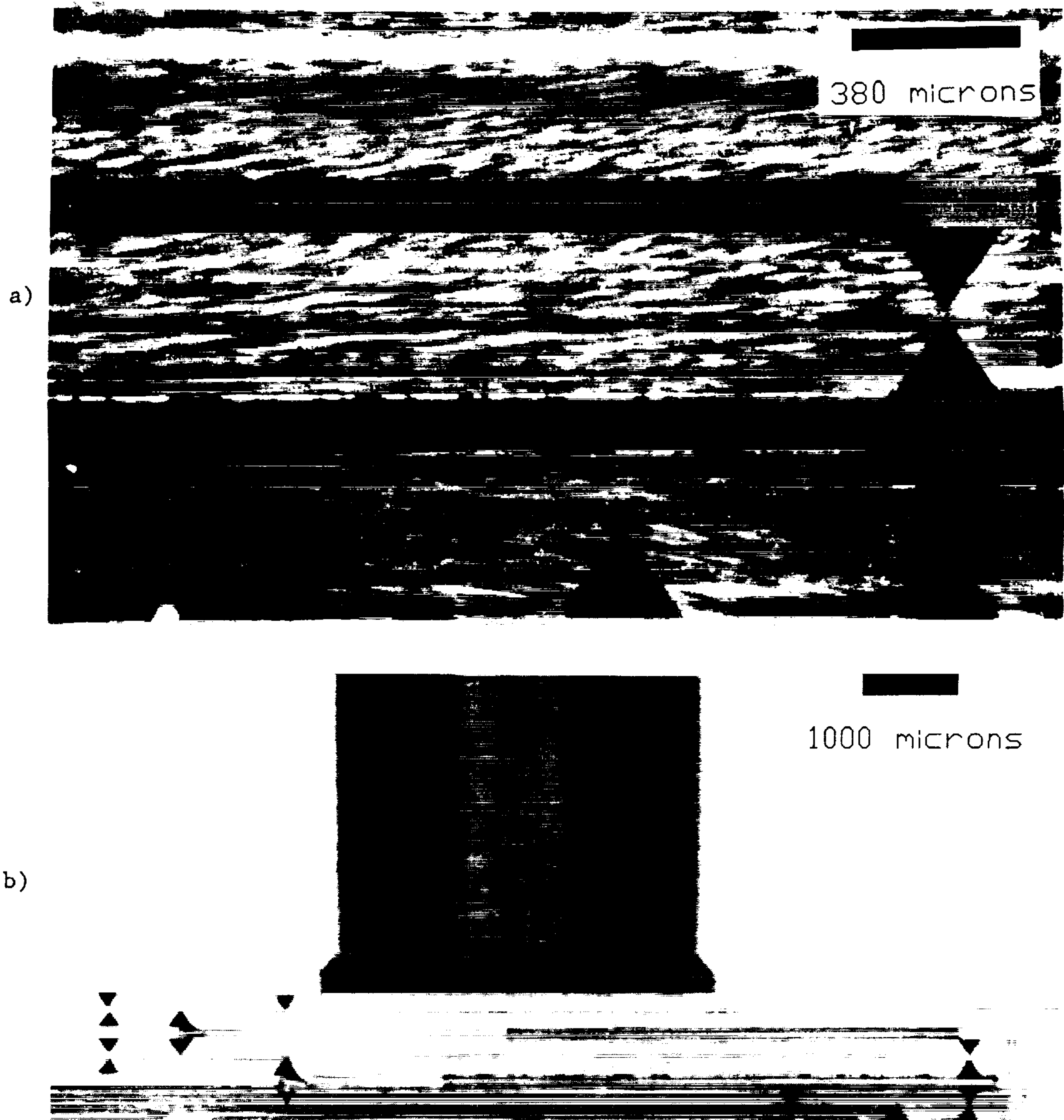

Figure 5

a) Optical micrograph of three silicon die stacked with glass fibers. V-grooves on right are to check infrared alignment, while the rest are for fibers. At present the overall structure's accuracy is limited by a $\pm 5\mu m$ infrared alignment of the die's top surface to its bottom surface.

b) Three silicon die will form an Einzel lens. The 0.16" vacuum pick up tool is visible in the micrograph showing the stack is self-supporting. The $2x10mm^2$ overhang of the die (Figure 2b) is rotated 90° between layers to facilitate electrical connections.

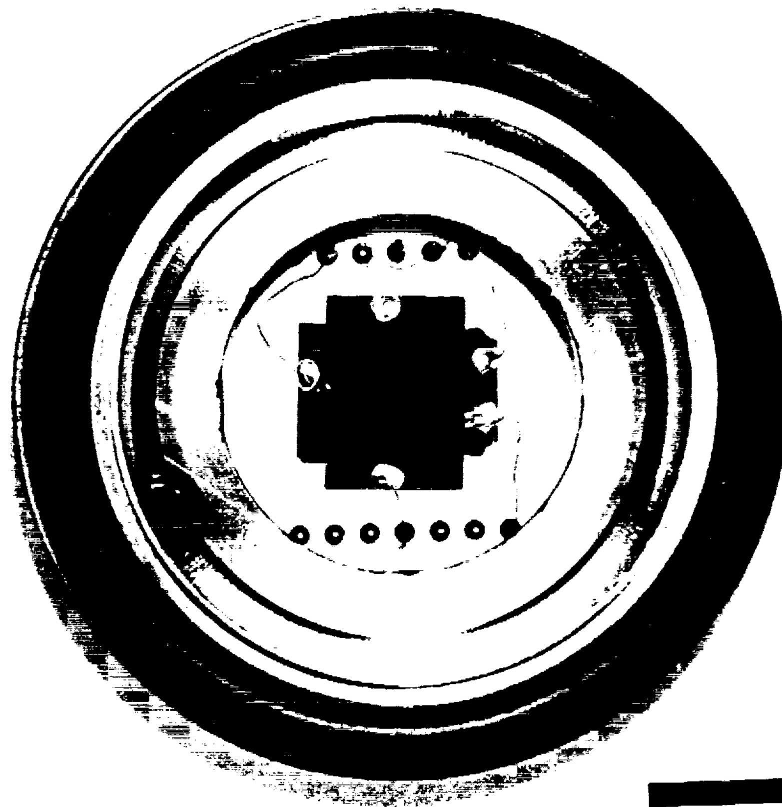

Figure 6

Four electrode stack mounted on an Airpax 1.1"x1.1" glass sealed 18 pin header. Two connections are made to the micromachined thermionic emitter on the bottom electrode. The header is seated into a 2.125" ISO quick-flange for mounting to vacuum test chamber. The structure is leak tight to 10^{-9} Torr.

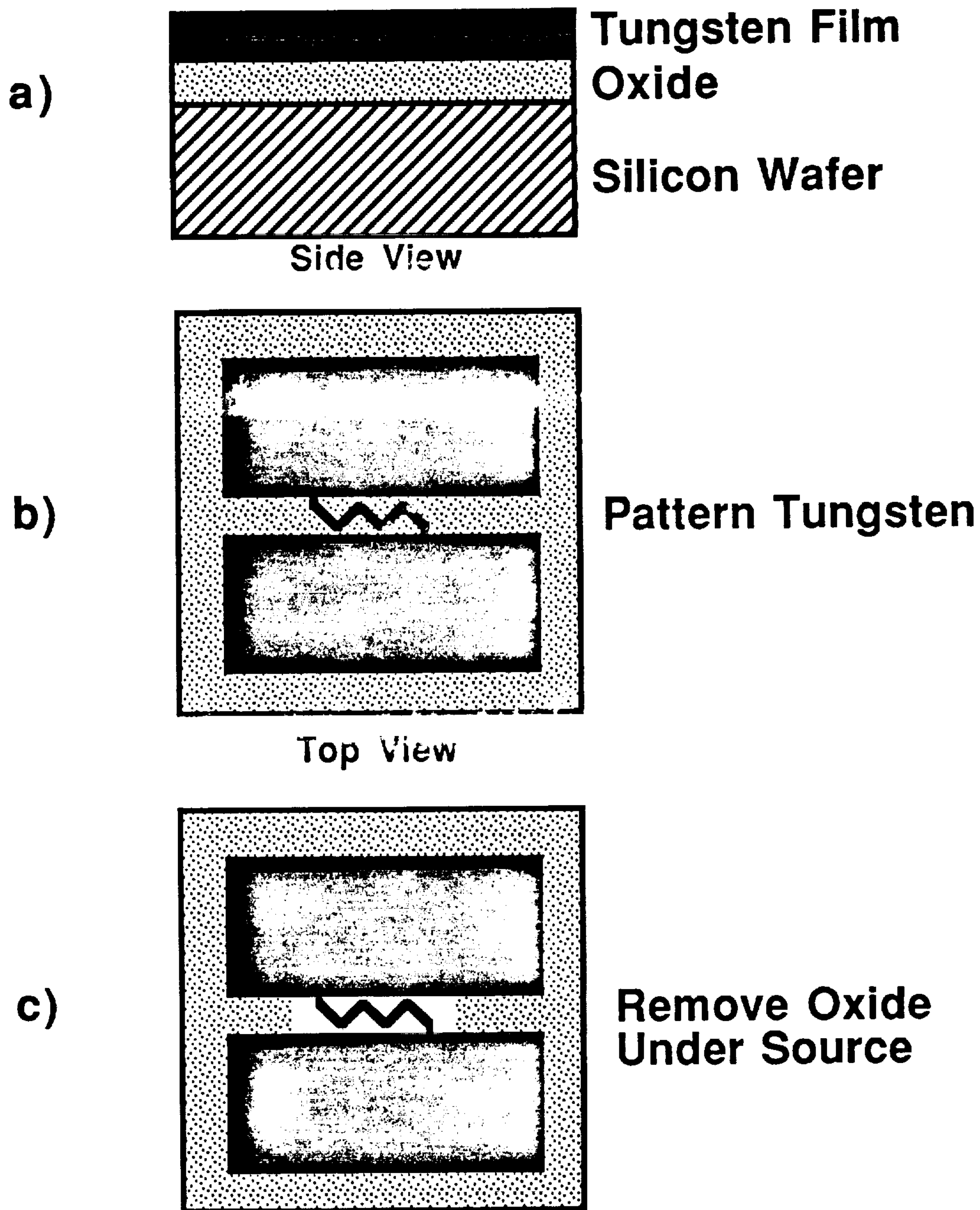

Figure 7

A Micromachined Thermionic Emitter.

a) A tungsten film is sputtered on an oxidized silicon wafer.

b) The tungsten film is photolithographically defined.

C) The oxide is removed from below the tungsten emitter and 10μm of exposed silicon is removed in KOH. The emitter can now be heated without interaction with the substrate.

a)

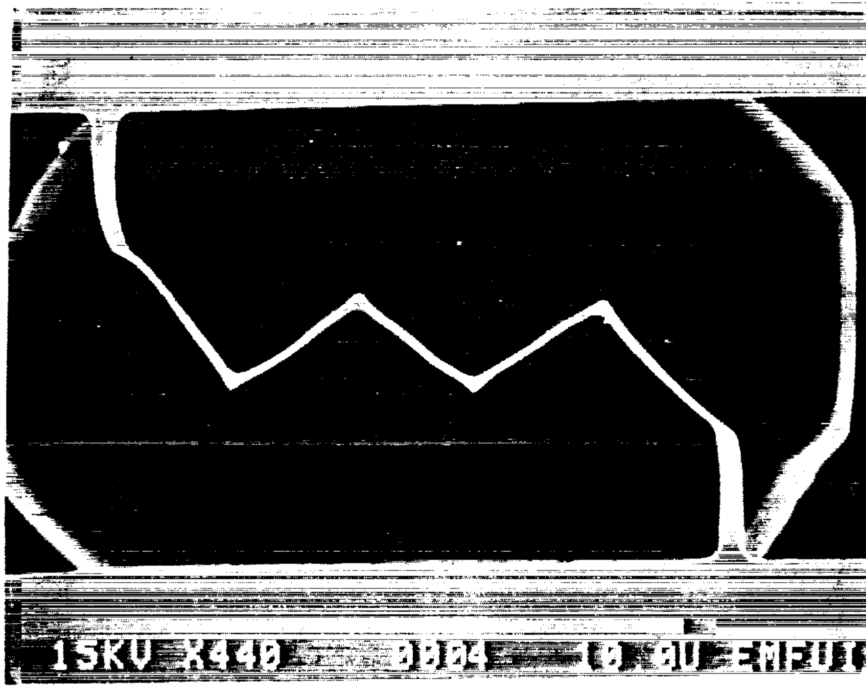

b)

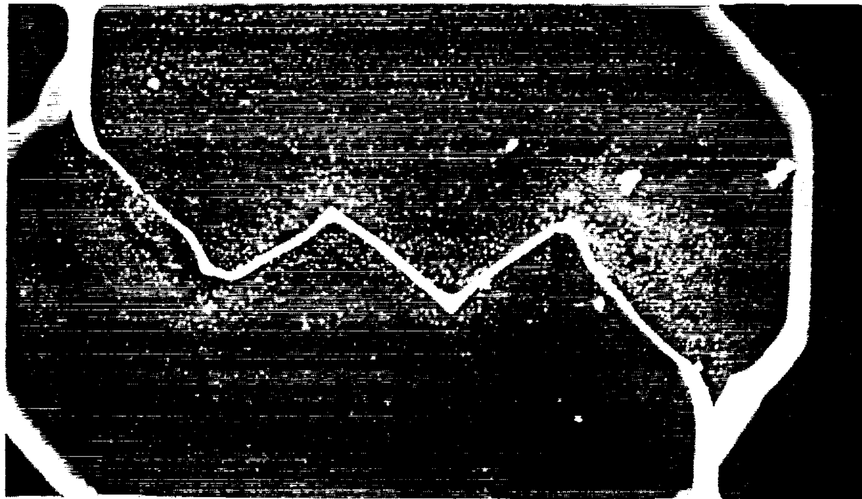

Figure 8

a) Electron micrograph of zigzag thermionic emitter prior to operation. Each section is $6 \times 50 \mu m^2$.
b) Electron micrograph of emitter after operation. The tungsten emitter is $.1 \mu m$ thick and emitted 10namps for 1 hour.

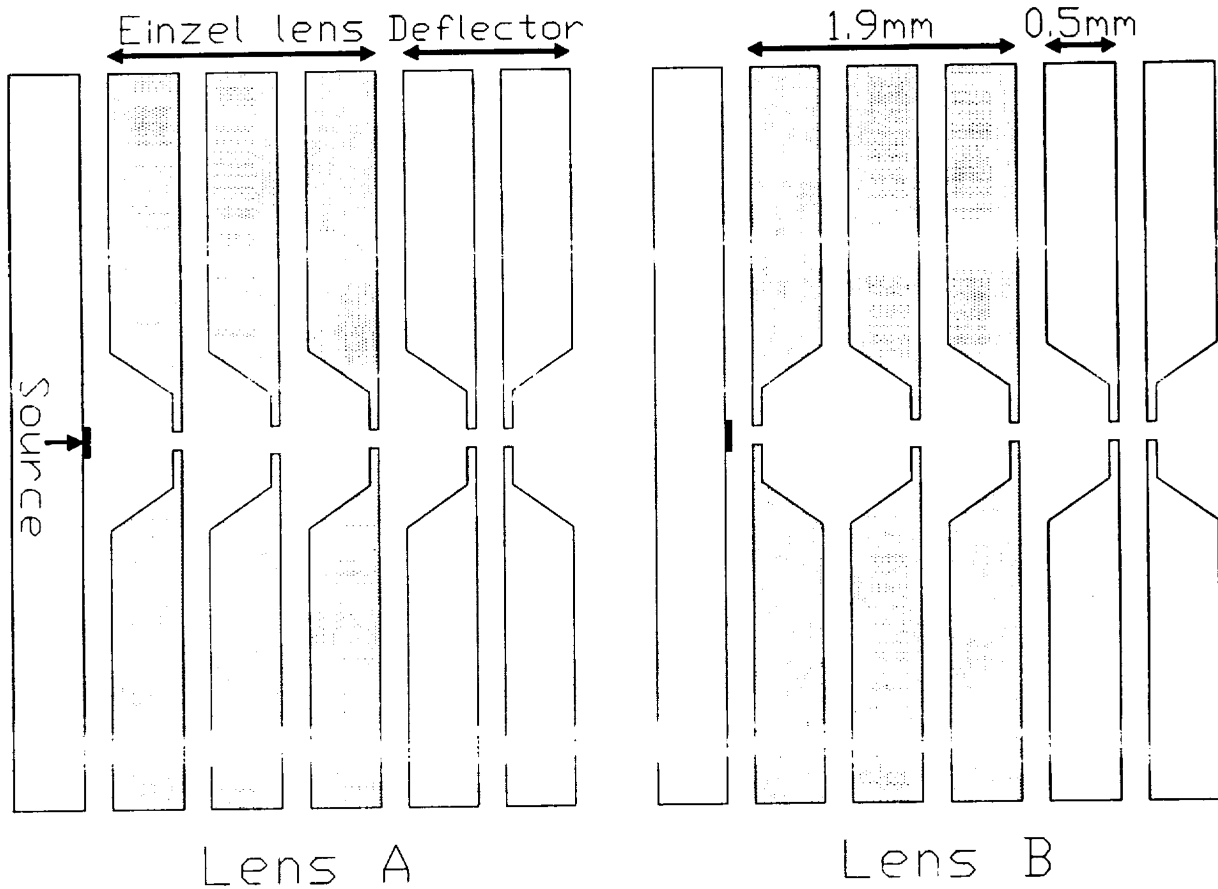

Figure 9

Two electron columns consisting of an electron source, Einzel lens, and deflectors were modeled. The Einzel lenses are shaded and the lenses differ only in the orientation of their first electrode. The first and third apertures are 100μm in diameter while the second aperture is 150μm. The gaps between the silicon electrodes are approximately 200μm. The focusing potential of the first electrode in the case of Lens B has an earlier and more gradual effect than in the case of Lens A.

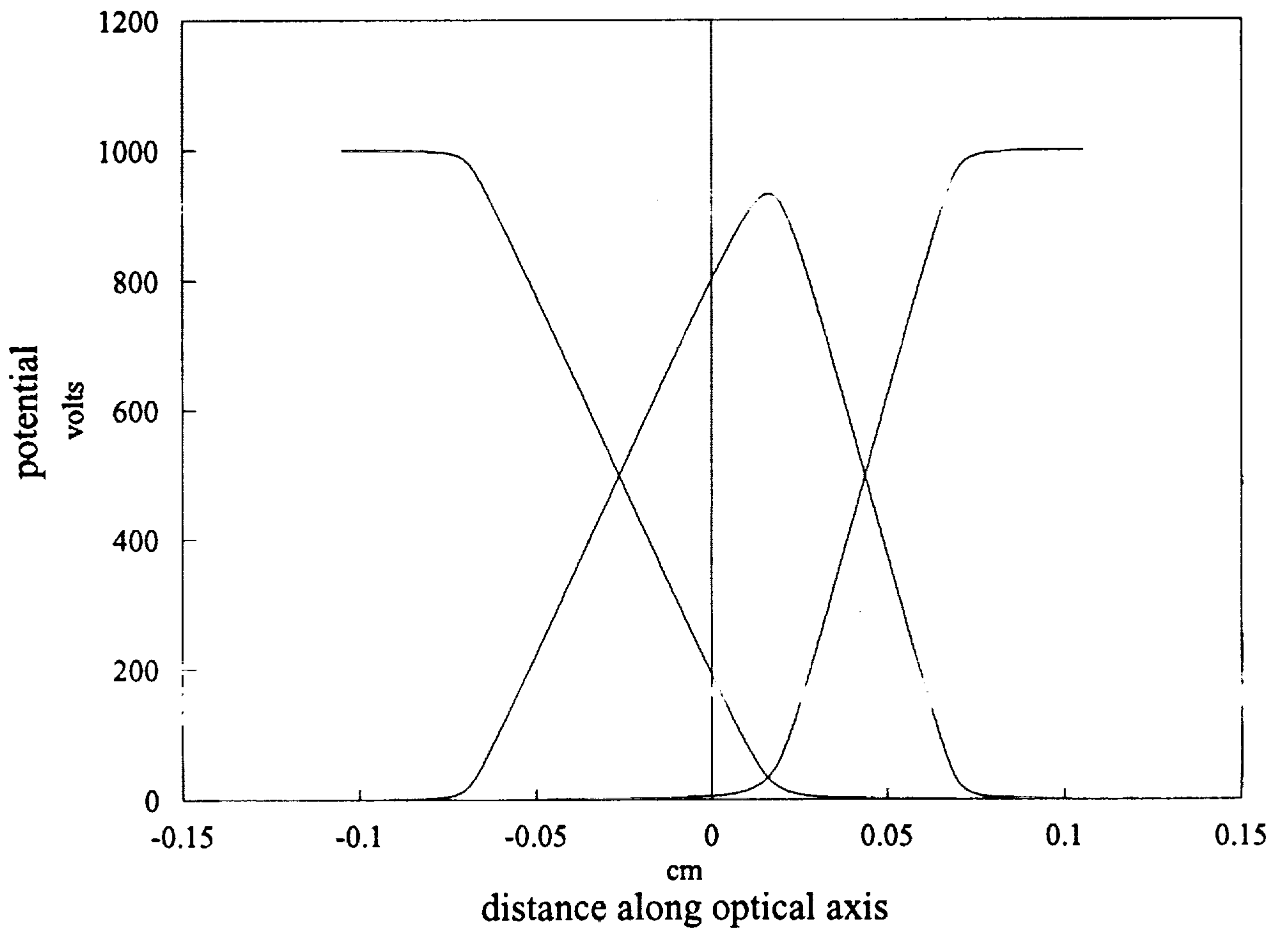

Figure 10

Individual electrode contributions to the axial potential for Lens B in Figure 9. The electrode potentials are normalized to 1 kV, a simple selectively scaled superposition of the individual contributions will provide the axial potential potential distribution for the lens.

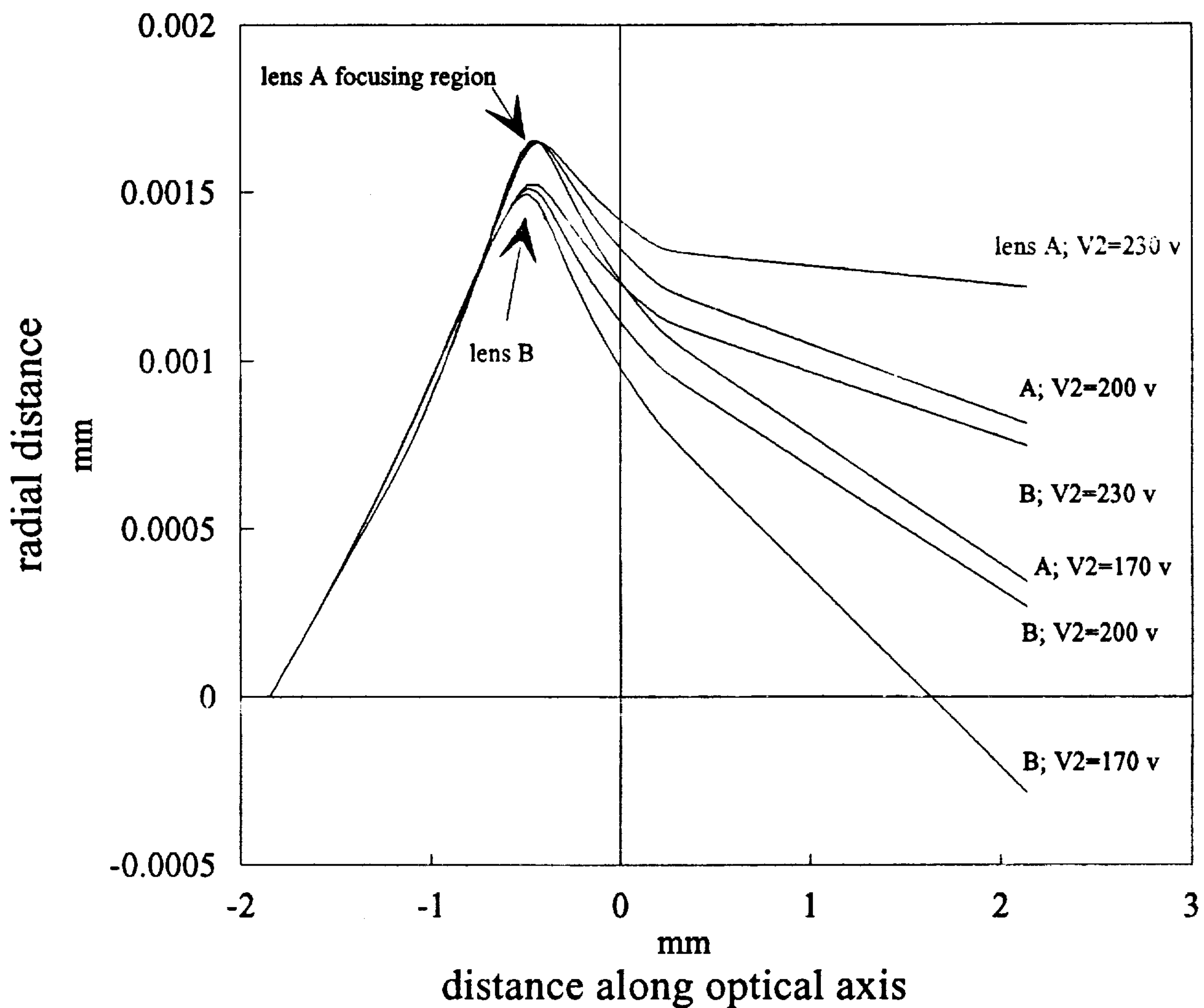

Figure 11

Ray trace comparison between the two micromachined three element Einzel lenses in Figure 9. The initial conditions for the fourth order Runga-Kutta ray trace routine are a point source on the axis with an initial angle of 1 mrad.

a)

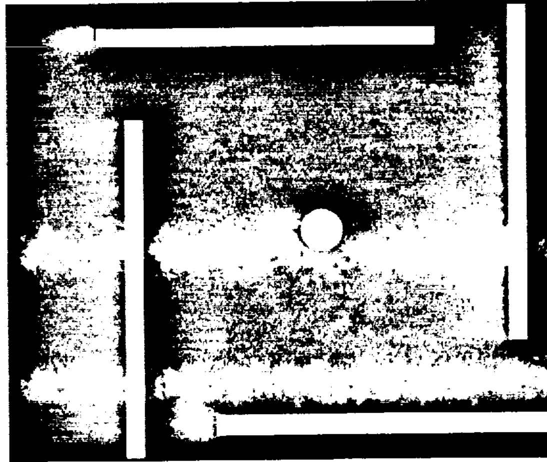

b)

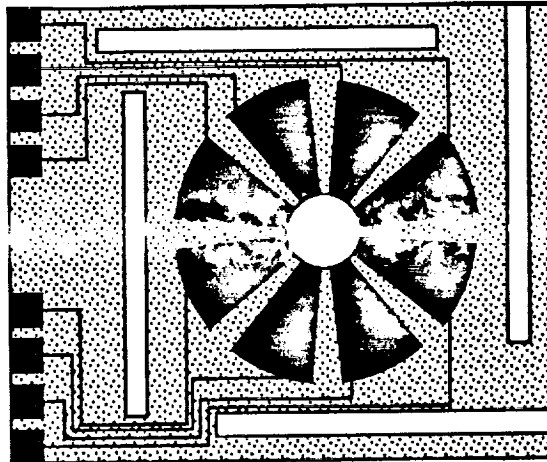

c)

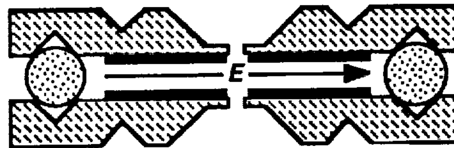

Figure 12

a) Both sides of each silicon die at a single potential will have a uniform coating of metal.
b) One of the silicon die used to deflect the electron beam and correct for astigmatism. Die has eight independently controlled metal electrodes insulated from the silicon with a thick high quality SiO_2 layer.
c) Cross-sectional view of deflector indicating the transverse electric field between the die.